

Computational Model of Cortical Bone Pore Water Frequency Distribution, T_2' and T_2^*

Cheng Li¹, Henry Ong², Alexander C. Wright¹, Shing Chun Benny Lam³, and Felix W. Wehrli¹

¹Laboratory for Structural NMR Imaging, Department of Radiology, University of Pennsylvania, Philadelphia, PA, United States, ²Vanderbilt University Institute of Imaging Science, Vanderbilt University, Nashville, TN, United States, ³Department of Psychiatry, University of Pennsylvania, Philadelphia, PA, United States

Introduction – Cortical bone water (BW) plays a pivotal role for transport of nutrients, mechanotransduction of signals from osteocytes to osteoblasts, and it is essential in conferring viscoelastic properties to bone. The dominant fraction of BW is bound to collagen, bone's major organic constituent. The remainder, referred to as pore BW, resides in the spaces of the Haversian and lacunocanalicular system (1). During aging and more so in osteoporosis, the Haversian system expands, resulting in increased pore volume fraction that is associated with decreased mechanical competence. Knowledge of the pore BW fraction is therefore of considerable interest (2). BW can be quantified by ultra-short TE (UTE) MRI (3) and it may be possible to separate the two fractions by fitting the FID signal decay to a sum of two exponentials with the longer component attributed to pore water on grounds that it is more mobile (T_2^* on the order of milliseconds as opposed to $\sim 300\mu\text{s}$ for bound water) (4). However, it has also been argued that pore water could also be short-lived due to frequency dispersion resulting from internal gradients (5) resulting from the susceptibility difference between bone and pore water. Here we examine this hypothesis by modeling the induced field from high-resolution μCT images as a means to estimate the decay rate of pore water.

Methods - Cortical Bone Specimen Preparation: A human cortical bone specimen was harvested from the tibial mid-shaft of a 65 year old female donor. Using a Dremel rotary tool (www.dremel.com), a $1\times 1\times 1\text{ mm}^3$ was sectioned for high-resolution μCT imaging.

μCT Image Acquisition: A 3D μCT image was acquired on a SkyScan 1172 (SkyScan, Kontich, Belgium) scanner at $1\mu\text{m}^3$ isotropic voxel size with the following parameters: 59 kV, 167 μA , 0.5 mm aluminum filter, 641 views, 0.3° increment, 1.5 s exposure, 12 averages, scan time 3 hrs 16 mins.

Pore BW Segmentation and Pore Surface-to-Volume Ratio Estimation: From the acquired μCT images, Haversian and Volkmann's canals and osteocyte lacunae were segmented by a two-step thresholding and morphological reconstruction operator approach. Finally, the background of the μCT image was filled in with bone material, assuming two susceptibility compartments are considered. After the segmentation, the marching cubes algorithm was used for surface tiling to estimate the surface/volume ratio (S/V) of each pore as a means to estimate pore water T_2 according to $1/T_2 \propto S/V$ (6).

Induced Field Calculation: From the segmented image, a 3D susceptibility map $\Delta\chi(x, y, z)$ was generated by assigning voxels classified as bone matrix and pore space a value of 0, and $4\pi\cdot 0.19$ ppm (SI units), respectively, matching reported susceptibility differences between bone and water (7). The induced magnetic field (in ppm) along the main field direction is given by (8):

$$\Delta B/B_0 = FT^{-1} \left(FT(\Delta\chi(x, y, z)) \left(\frac{1}{3} - \frac{(k_x \cos\theta - k_y \sin\theta)^2}{k_x^2 + k_y^2 + k_z^2} \right) \right) [1]$$

where FT denotes the Fourier transform operator, k -space coordinates (k_x, k_y, k_z) are defined with respect to the object, and θ is the angle by which the external magnetic field B_0 is clockwise rotated about the x -axis. To examine the orientation dependence, the induced fields at θ s of 0° , 50° and 90° were simulated. B_0 was set to 3T for all simulations.

Pore BW Relaxation Time Estimation: The FID from a $0.5\times 0.5\times 0.5\text{ mm}^3$ VOI to mimic a typical voxel in a UTE imaging experiment was computed in two ways. First, to gain insight into T_2^* , i.e. relaxation solely from the distribution of induced fields, the FID was calculated as $s(t) = \sum_i \exp(j2\pi\gamma\Delta B_i t)$ with echo time t ranging from $10\mu\text{s}$ to 200 ms in $50\mu\text{s}$ steps. Second, the total

FID signal, i.e. $1/T_2^* = 1/T_2' + 1/T_2$, was calculated as $s(t) = \sum_i \exp(-\frac{t}{T_{2,i}} + j2\pi\gamma\Delta B_i t)$,

where $T_{2,i}$ of each pore was based on its S/V ratio. As the proportionality constant is unknown, each S/V was mapped to a T_2 to range from 1 to 10ms. In all calculations, the static dephasing regime is assumed. In addition, frequency histograms were computed from 3D maps of the induced field. To estimate T_2^* , the FID signals were analyzed with the aid of the Multi-Exponential Relaxation Analysis (MERA) toolbox (9) via regularized non-negative least-squares (NNLS) fitting. All the computations were performed with MATLAB (Mathworks, Natick, MA, USA).

Results - Fig. 1 displays (a) 3D rendition of a high-resolution μCT volume of cortical bone specimen showing Haversian and Volkmann's canals (red) and osteocyte lacunae (blue), (b) image slice from the volume data set, (c) corresponding segmented binary image, (d) simulated induced field map at tilt angle of 0° (parallel to B_0). Fig.2 shows (a) histograms of the induced field, (b) predicted FID signal due to T_2' , (c) predicted total FID signal due to T_2^* and (d) the T_2^* spectra of the pore water at tilt angles of 0° , 50° and 90° . As the direction of the main field changes, frequency shift is observed reflecting the change in the orientation of Haversian canals where most pore water resides. The T_2^* s of the pore water were found as 5.5 ms at 0° , 4.1 ms at 50° and 4.6 ms at 90° , which are of the same order as the experimentally measured values reported by Du. et al. (4).

Discussion & Conclusions - Our preliminary results show that the internal gradients resulting from the susceptibility difference between bone and pore water shortens the pore water T_2^* , but the predicted T_2^* values are still well discernible from bound water. The simulation results may lend some credence to the separability of pore and bound water based on the hypothesis that $T_{2\text{bound}} \ll T_{2\text{pore}}$. However, since only one cortical bone specimen was examined in the simulation and actual T_2 values of the pores in the sample volume are unknown, further investigations on more specimen samples are needed along with experimental verification.

References: 1. Ong H. et al. JBMR 2012 (in press); 2. Seeman E et al. N Eng J Med 2006; 354:2250-2261; 3. Techawiboonwong et al. Radiology 248:824 (2008). 4. Du J et al. MRM 2012 (in press); 5. Horch A. et al. MRM 2012 (in press); 6. Brownstein K.R. et al. Physical Review 1979:19(6)2446; 7. Hopkins J.A. et al. MRM 1997;37(4):494-500; 8. Marques J.P. et al. Concepts in Magnetic Resonance Part B 2005;25B(1):65-78; 9. Does M, et al. http://www.vuiis.vanderbilt.edu/~doesmd/MERA/MERA_Toolbox.html.

Acknowledgements: NIH RO1 AR50068, HHMI International Student Research Fellowship. We thank Drs. Tatiparthi and Sledz for acquiring the μCT image.

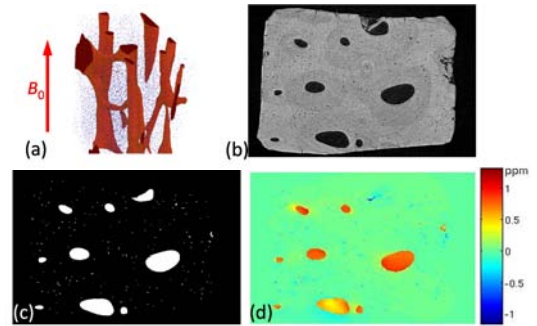


Fig. 1 3D rendering (a), image slice (b), binary image (c) and field map (d)

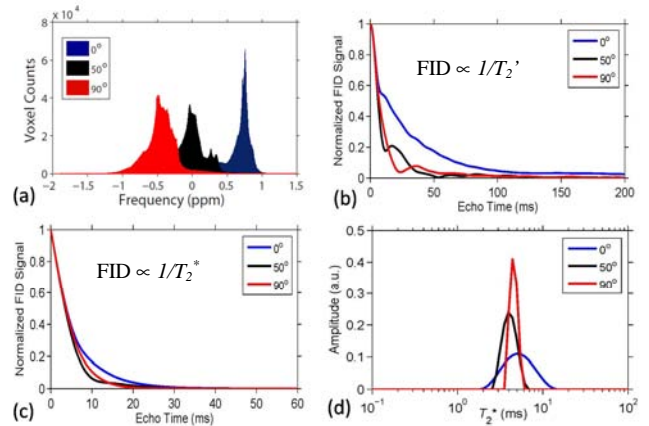


Fig. 2 Frequency histogram(a), FID signals(b, c) and T_2^* spectrum(d)